

# Aquifer-scale mapping of injection capacity for potential aquifer storage and recovery sites: Methodology development and case studies in Minnesota, USA



Raghwendra N. Shandilya <sup>a,b</sup>, Etienne Bresciani <sup>a,c</sup>, Anthony C. Runkel <sup>d</sup>,  
Carrie E. Jennings <sup>e</sup>, Seunghak Lee <sup>a,b,f,\*</sup>, Peter K. Kang <sup>g,h,\*\*</sup>

<sup>a</sup> Water Cycle Research Center, Korea Institute of Science and Technology (KIST), Seoul, South Korea

<sup>b</sup> KIST School, Korea University of Science and Technology (UST), Seoul, South Korea

<sup>c</sup> Center for Advanced Studies in Arid Zones (CEAZA), La Serena, Chile

<sup>d</sup> Minnesota Geological Survey, University of Minnesota, St. Paul, MN, USA

<sup>e</sup> Freshwater Society, St. Paul, MN, USA

<sup>f</sup> Graduate School of Energy and Environment (KU-KIST Green School), Korea University, Seoul, South Korea

<sup>g</sup> Department of Earth and Environmental Sciences, University of Minnesota, Minneapolis, MN, USA

<sup>h</sup> Saint Anthony Falls Laboratory, University of Minnesota, Minneapolis, MN, USA

## ARTICLE INFO

### Keywords:

Aquifer storage and recovery  
Injection capacity  
Mapping  
Water security  
Minnesota

## ABSTRACT

**Study Region.** Two areas in Minnesota, USA: Buffalo aquifer in Clay County and Jordan aquifer in Olmsted County. There are concerns about the long-term sustainability of groundwater resources in the two aquifers. **Study Focus.** Aquifer storage and recovery is an important tool for water resources management in various geographic and socio-economic contexts. However, practical guidelines regarding the assessment of injection capacity remain limited. In this study, we present a quantitative methodology which is based on the Theis solution. The methodology allows an efficient estimation of well-based injection capacity and generation of an aquifer-scale injection capacity map. We present a detailed workflow for applying the methodology and demonstrate its application to the two study areas. The tool developed in this study can be easily applied to other areas. **New Hydrological Insights for the Region.** The two study areas show significant spatial variability in injection capacity. In the Buffalo aquifer, the variability is mainly controlled by transmissivity, whereas in the Jordan aquifer, it is mainly controlled by maximum allowable hydraulic head change. Assuming an injection duration of one month and considering the 90-percentile value of the injection capacity at each site, we found that two and four wells are required to inject the volume of water equivalent to one month of domestic water requirements for the cities of Moorhead and Rochester, respectively.

## 1. Introduction

Groundwater constitutes the largest unfrozen freshwater reserve on the earth (Aeschbach-Hertig and Gleeson, 2012; Shiklomanov

\* Corresponding author at: Water Cycle Research Center, Korea Institute of Science and Technology (KIST), Seoul, South Korea.

\*\* Corresponding author at: Department of Earth and Environmental Sciences, University of Minnesota, Minneapolis, MN, USA.

E-mail addresses: [seunglee@kist.re.kr](mailto:seunglee@kist.re.kr) (S. Lee), [pkkang@umn.edu](mailto:pkkang@umn.edu) (P.K. Kang).

<https://doi.org/10.1016/j.ejrh.2022.101048>

Received 26 August 2021; Received in revised form 7 February 2022; Accepted 25 February 2022

Available online 28 February 2022

2214-5818/© 2022 The Authors. Published by Elsevier B.V. This is an open access article under the CC BY-NC-ND license (<http://creativecommons.org/licenses/by-nc-nd/4.0/>).

and Rodda, 2003). It supplies drinking water to nearly 2.5 billion people (Grönwall and Danert, 2020), and more than 38% of the globally irrigated areas rely on groundwater (Siebert et al., 2010). In many agrarian regions of the world, groundwater has been instrumental in accelerating economic and social development, contributing to food security and poverty alleviation (Gleeson et al., 2010; Roy and Shah, 2002). The dependence on groundwater will continue to increase to meet the needs of increasing world population, maintain food security, and sustain economic and social development. Despite its critical importance, groundwater resources in many parts of the world are insufficiently managed and are experiencing unsustainable exploitation (Famiglietti, 2014; Famiglietti and Rodell, 2013; Rodell et al., 2009). Additionally, many regions are affected by climate change, which further complicates the management of groundwater due to its uncertain impacts on water resources (Collins et al., 2013; Famiglietti, 2014; Wu et al., 2020).

In the midst of these challenges, various water management practices have been proposed and employed across the globe to increase the sustainability of water resources (Kim et al., 2017; Onderka et al., 2020; Rockström and Falkenmark, 2015). However, many of these efforts are focused on the construction of dams and reservoirs for increasing surface water storage, which requires large financial costs, cause significant water losses by evaporation, and have significant sociological and ecological impacts (Alazard et al., 2015; Craig et al., 2005; Mailhot et al., 2018; Mumba and Thompson, 2005). Among alternative water management practices, managed aquifer recharge (MAR), which involves the purposeful recharge of water to aquifers, has gained increased interest globally (Dillon et al., 2019). MAR is the umbrella term for several techniques such as aquifer storage and recovery (ASR), pond infiltration, bank filtration, and rainwater harvesting (Dillon, 2005).

In the ASR method, water is injected into an aquifer through well(s) at the time of availability, and recovered from the same well(s) when there is an increase in water demand (Pyne, 2005). ASR has various advantages such as reduction in evaporation losses, land requirements, and costs as compared to traditional surface storage structures (Bouwer, 2002; Khan et al., 2008; Maliva et al., 2006). ASR is highly adaptable and applicable because water can be secured at target locations by constructing and managing wells, and many successful ASR implementations have been reported across the world (Bloetscher et al., 2014; Dillon et al., 2019; Kang et al., 2019; Stefan and Ansems, 2018; Zuurbier et al., 2014).

For successful implementation of an ASR project, one needs to assess the suitability of potential ASR sites. A site suitability study should address both the injection capacity, which is the maximum volume of water that can be injected, and recovery efficiency, which is the recovery percentage of the injected water. Of these two aspects, the estimation of injection capacity should be the first step because the ability to inject a sufficient volume of water is required *a priori* to ensure a sufficient recoverable volume. This step is the focus of this paper. The most common practice for site suitability assessment has been the development of site suitability index maps using multicriteria decision analysis (MCDA) (Brown et al., 2005; Russo et al., 2015; Smith et al., 2017). MCDA involves evaluating and combining various surface, subsurface and operational parameters. A rank is assigned to each parameter value based on a qualitative assessment, and a weight is given to each parameter. Both the ranking and weighting of the parameters are subjective, and thus there can be large variations in final results (Sallwey et al., 2019). As a result, the index maps produced with this type of approach are only qualitative and their reliability can be variable.

Despite the critical importance, only a few studies investigated the injection capacity of potential ASR sites based on a quantitative assessment (Dudding et al., 2006; Gibson et al., 2018; Hodgkin, 2004; Neumann, 2012). To our knowledge, there has been only one peer-reviewed article on this topic (Gibson et al., 2018). However, the work by Gibson et al. (2018) does not allow continuous aquifer-scale mapping of injection capacity, and confined and unconfined aquifers are not distinguished in their methodology. Further, we currently lack a systematic workflow for estimating well-based injection capacity and have a limited understanding of how various hydrogeological and operational parameters affect injection capacity. This study bridges these knowledge gaps by providing and applying a comprehensive workflow that efficiently produces continuous aquifer-scale injection capacity map.

The main objectives of this study are: 1) to propose a quantitative methodology that enables the aquifer-scale mapping of well-based injection capacity for both confined and unconfined aquifers, 2) to present the estimation procedure of input parameters that are required for injection capacity calculation, 3) to demonstrate the methodology by applying it two aquifers in Minnesota, USA, and producing aquifer-scale injection capacity maps. We also discuss the estimated injection capacity values with regard to the water demand of the studied area.

In Section 2, we present the methodology for estimating well-based injection capacity and comprehensively discuss the estimation procedure of five key input parameters. In Section 3, we introduce the two study areas and discuss their physical settings and hydrogeology. In Section 4, we present the results of the methodology applied to these areas. We then analyze the significance of estimated injection capacity values in terms of domestic water requirements and discuss the advantages and limitations of the proposed methodology. Finally, we provide conclusions in Section 5.

## 2. Methodology for aquifer-scale mapping of well-based injection capacity

### 2.1. Overview

In this study, we define injection capacity as the maximum volume of water that can be injected into an aquifer using a well pumped at a constant rate for given operational parameters (i.e., injection duration and well radius) under the constraint of a maximum allowable hydraulic head change. To estimate injection capacity, we need to determine the optimal injection rate that maximizes the injection capacity of a well over an injection duration. We start with the Theis (1935) solution, which is valid for homogeneous and non-leaky confined aquifers of infinite extent, constant-rate injection, fully-penetrating well, negligible skin layer, and negligible wellbore storage. Under these simplifying assumptions of Theis (1935), the hydraulic head change at a point in space and time is given as:

$$\Delta h(r, t) = \frac{Q}{4\pi T} E_1 \left( \frac{r^2 S}{4Tt} \right) \quad (1)$$

where  $E_1$  is the exponential integral function (also known as well function), defined by:

$$E_1(u) = \int_u^\infty \frac{e^{-x}}{x} dx \quad (2)$$

where  $u = \frac{r^2 S}{4Tt}$ . All the variables used in this study are defined in [Table 1](#).

At any time during the injection process,  $\Delta h$  is larger at the well than at any other point in the aquifer. Therefore, it is at the injection well that the maximum allowable hydraulic head change ( $\Delta h_{\max}$ ) will first be reached. We discuss the estimation procedure for  $\Delta h_{\max}$  in [Section 2.2.1](#). The  $\Delta h$  increases with increasing  $Q$  and  $t$ , and the optimal injection rate ( $Q_{\max}$ ) that maximizes injection capacity will be the one for which  $\Delta h = \Delta h_{\max}$  at the injection well is reached at the end of the injection period (i.e.,  $t = t_{\text{inj}}$ ; orange line in [Fig. 1](#)). Any other values of  $Q$  (either  $Q > Q_{\max}$  or  $Q < Q_{\max}$ ) will lead to the non-optimal value of the injection capacity.  $Q < Q_{\max}$  will lead to the underutilization and  $Q > Q_{\max}$  will lead to problems like well overflow and the fracturing of a confining unit. This statement for  $\Delta h_{\max}$  at  $t = t_{\text{inj}}$  can be expressed as the following equation:

$$\Delta h_{\max} = \frac{Q_{\max}}{4\pi T} E_1 \left( \frac{r_w^2 S}{4Tt_{\text{inj}}} \right) \quad (3)$$

Solving for  $Q_{\max}$  gives:

$$Q_{\max} = \frac{4\pi T \Delta h_{\max}}{E_1 \left( \frac{r_w^2 S}{4Tt_{\text{inj}}} \right)} \quad (4)$$

The injection capacity ( $V_{\max}$ ) is then given by:

$$V_{\max} = Q_{\max} \times t_{\text{inj}} = \frac{4\pi T \Delta h_{\max} t_{\text{inj}}}{E_1 \left( \frac{r_w^2 S}{4Tt_{\text{inj}}} \right)} \quad (5)$$

The above equation is the basis of the quantitative methodology that enables the aquifer-scale mapping of well-based injection capacity.

**Table 1**  
Nomenclature.

Symbol	Definition
ATE	aquifer-top elevation (L)
D	depth to the bottom of confining layer (L)
$E_1$	exponential integral function
$g$	acceleration due to gravity ( $L T^{-2}$ )
GSE	ground surface elevation (L)
$h_0$	initial hydraulic head (L)
$h_{\max}$	allowable hydraulic head (L)
$h_p$	pore water pressure head (L)
$h_{ap}$	allowable pressure head (L)
$h_{fp}$	fracture pressure head (L)
$\Delta h$	hydraulic head change (L)
$\Delta h_{\max}$	maximum allowable hydraulic head change (L)
K	hydraulic conductivity ( $L T^{-1}$ )
$p_o$	atmospheric pressure ( $M^1 L^{-1} T^{-2}$ )
Q	injection rate ( $L^3 T^{-1}$ )
$Q_{\max}$	maximum injection rate ( $L^3 T^{-1}$ )
r	distance from the well to the evaluation point (L)
$r_w$	well radius (L)
S	storativity (–)
SF	safety factor (–)
SL	safety limit (L)
t	time (T)
$t_{\text{inj}}$	injection duration (T)
T	aquifer transmissivity ( $L^2 T^{-1}$ )
u	dimensionless parameter (–)
$V_{\max}$	injection capacity ( $L^3$ )
$\rho_w$	density of water ( $ML^{-3}$ )
$\rho_o$	bulk density of overburden material ( $ML^{-3}$ )
v	Poisson ratio of overburden material

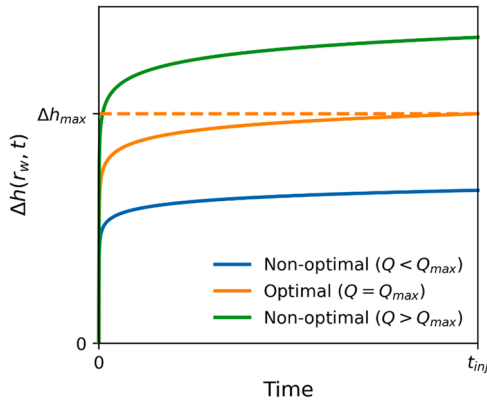


**Fig. 1.** Illustration of an optimal injection rate that maximizes injection volume based on the Theis principle.  
Adapted from Shandilya et al. (2022).

## 2.2. Key parameters for injection capacity calculation

The equation for an injection capacity of a well (Eq. (5)) has five input parameters:  $\Delta h_{\max}$ ,  $T$ ,  $t_{\text{inj}}$ ,  $S$ , and  $r_w$ . In this section, we present the estimation procedure for these parameters. The estimation procedure varies between unconfined and confined aquifers (Fig. 2a and Fig. 2b), and a workflow chart (Fig. 2c) shows various factors that control the five input parameters and how they are combined to determine injection capacity.

### 2.2.1. Maximum allowable hydraulic head change

Maximum allowable hydraulic head change ( $\Delta h_{\max}$ ) is the permissible hydraulic head increase at an injection well such that the head increase does not cause undesirable effects such as ground surface flooding, flowing artesian wells, or fracturing of confining units. The estimation procedure for  $\Delta h_{\max}$  is different between unconfined and confined aquifers (Fig. 2a and Fig. 2b); flooding is a major risk for unconfined aquifers and fracturing of a confining layer is a major risk for confined aquifers. In the following, we discuss  $\Delta h_{\max}$  calculations for unconfined and confined aquifers separately.

In unconfined aquifers, the major risk associated with injection is waterlogging or flooding near an injection well.  $\Delta h_{\max}$  for injection in unconfined aquifers is the difference between the ground surface elevation (GSE) and the initial (before the start of injection operation) hydraulic head ( $h_0$ ). After factoring in a safety limit ( $SL$ ),  $\Delta h_{\max}$  for an unconfined aquifer can be expressed as:

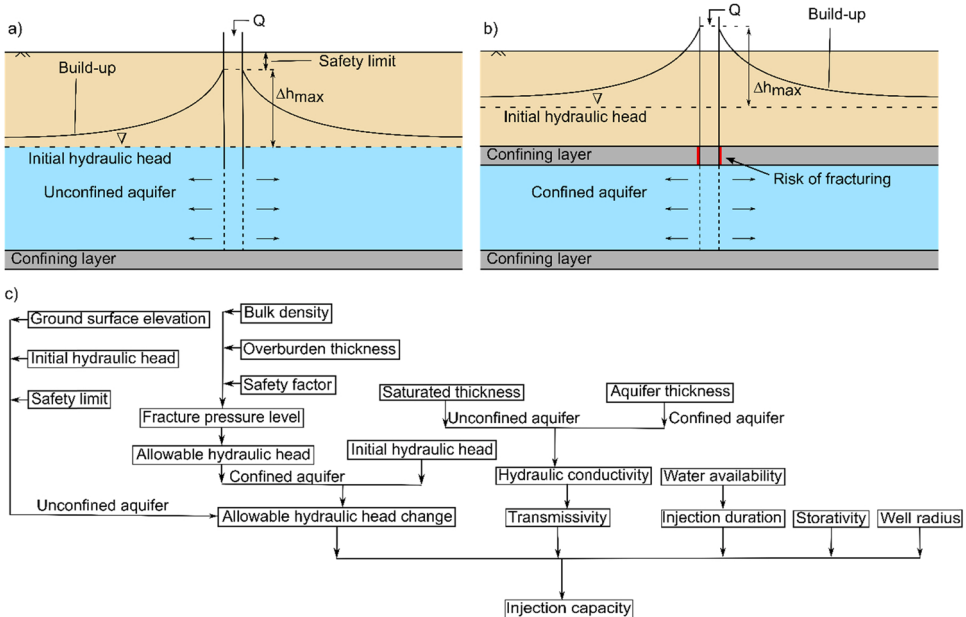


**Fig. 2.** Schematics illustrating the concept of maximum allowable hydraulic head change for (a) unconfined and (b) confined aquifers. (c) Workflow chart showing how various parameters are combined to estimate an injection capacity of a well.

$$\Delta h_{\max} = (GSE - SL) - h_0 \quad (6)$$

The criteria for selecting the value of  $SL$  should be specific to the site context. For injection wells located in an open field or farmland, one should mostly be concerned about the depth equivalent to the soil root zone so that the increase in groundwater level does not cause harm to plants. For an open agricultural area with few settlements, we propose an  $SL$  value of 2.5 m below ground surface, which, in most cases, will exclude the soil root zone (Fan et al., 2016; Schenk and Jackson, 2002). If the injection wells are located near settlements or urbanized locations, the value of  $SL$  should be selected more conservatively and in accordance with the depth of basements and building foundations, which is normally deeper than the soil root zone. For this scenario, one may use 5 m for  $SL$  (Dudding et al., 2006; Hodgkin, 2004). Note that most areas except those very close to an injection well will have headspace significantly larger than  $SL$  because hydraulic head decreases rapidly from an injection well.

In confined aquifers,  $\Delta h_{\max}$  is essentially constrained by the fracture pressure of the upper confining layer. Thus, the injection pressure of a well should always be lower than the amount of pressure that the upper confining layer can withstand without generating fractures. For aquifer storage purposes, the fracture pressure head ( $h_{fp}$ ) can be estimated using the thickness and bulk material density of each layer present above an aquifer (Szulczeński et al., 2012; Zoback, 2007). Another important point to consider before calculating  $h_{fp}$  is the stress regime in the area (Szulczeński et al., 2012). The calculation procedure varies depending on the stress regime, which governs the orientation of least principal stress. Both study sites have the least principal stress oriented in the horizontal direction (Levandowski et al., 2018). When the least principal stress is oriented in the horizontal direction, the expression for the fracture pressure head can be obtained as:

$$h_{fp} = \sum_{i=1}^n \left( \left( \frac{v_i}{1-v_i} \right) \times \left( \frac{\rho_{oi} D_i}{\rho_w} - h_{pi} \right) + h_{pi} + \frac{p_o}{\rho_w g} \right) \quad (7)$$

where  $n$  is the number of overlying layers with different bulk density values. By incorporating safety factor ( $SF$ ) in the calculation, we obtain the allowable pressure head ( $h_{ap}$ ) above the aquifer-top elevation as:

$$h_{ap} = h_{fp} \times (1 - SF) \quad (8)$$

For example, if we use a 15% safety factor,  $h_{ap}$  in the injection well is at 85% of  $h_{fp}$ . Finally, the expression for allowable hydraulic head ( $h_{\max}$ ) in a confined aquifer can be obtained by summing  $h_{ap}$  and aquifer-top elevation (ATE):

$$h_{\max} = ATE + h_{ap} \quad (9)$$

With  $h_{\max}$  and  $h_0$ ,  $\Delta h_{\max}$  for a confined aquifer can then be obtained as:

$$\Delta h_{\max} = h_{\max} - h_0 \quad (10)$$

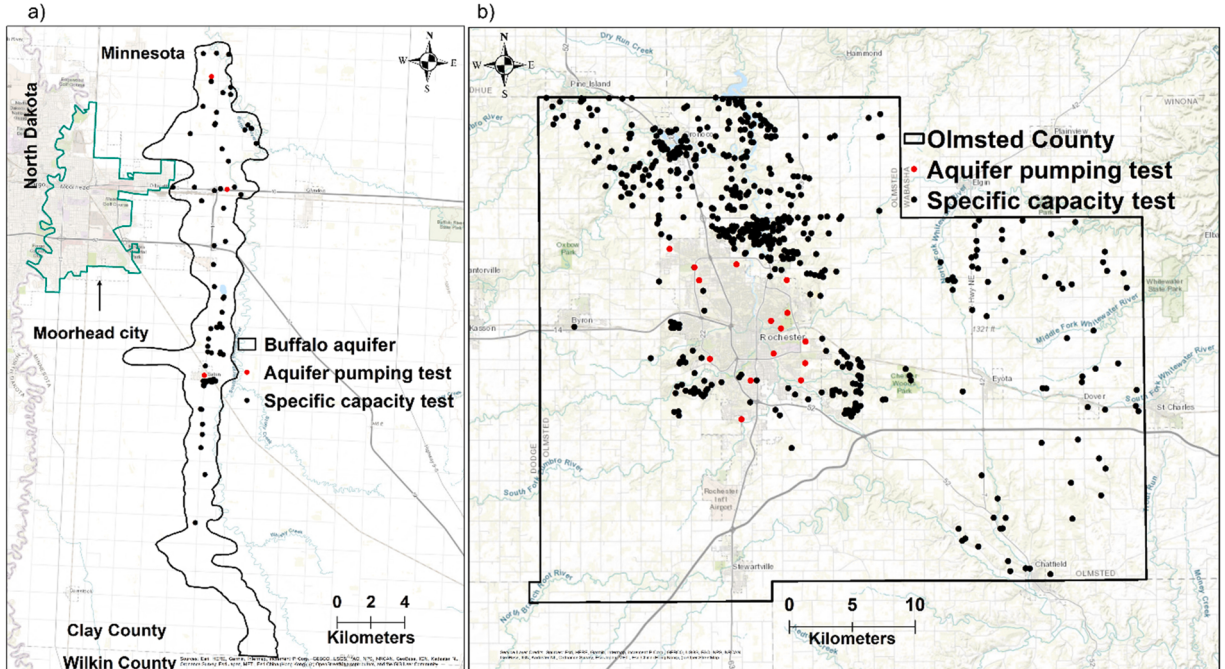


**Fig. 3.** Maps showing the locations of aquifer pumping tests and specific capacity tests in (a) Buffalo aquifer, Clay County, and (b) Olmsted County.

### 2.2.2. Transmissivity

Transmissivity ( $T$ ) is a key hydrogeologic parameter that controls the injection capacity, and  $T$  estimates can often be obtained from aquifer pumping and specific capacity tests. For injection capacity estimations,  $T$  should ideally be estimated from aquifer pumping tests with a duration equivalent to the target injection duration at target locations. However, performing such long-term tests is expensive and uncommon. Thus, specific capacity test (Ahmed and De Marsily, 1987; Bradbury and Rothschild, 1985; Richard et al., 2016) along with aquifer pumping test are used to estimate  $T$ . In this study, we use the method proposed by Bradbury and Rothschild (1985) to estimate  $T$  from specific capacity tests. We use  $T$  values obtained from aquifer pumping tests for locations where both pumping and specific capacity test data are available because a long-duration test provides a more representative  $T$  value compared to a typical specific capacity test (Richard et al., 2016). For the Buffalo aquifer, we used aquifer pumping test data from 4 locations (Schoenberg, 1998) and specific capacity test data from 76 locations (Fig. 3a). For the Jordan aquifer, we used aquifer pumping test data from 15 locations and specific capacity test data from 593 locations (Fig. 3b).

To generate a  $T$  map, one may want to directly interpolate the punctual  $T$  values using, for example, a geostatistical method. However,  $T$  depends both on hydraulic conductivity ( $K$ ) and saturated thickness, and, at the regional scale, these two parameters may follow different spatial patterns resulting from different processes. Hence, to generate a  $T$  map, we first generate a  $K$  map (geostatistical interpolation of the punctual  $K$  values), and then we multiply it by a saturated thickness map. The saturated thickness is taken equal to the aquifer thickness where the aquifer is confined, and to the saturated portion of the aquifer thickness where the aquifer is unconfined. From the  $T$  map thus obtained, we perform a spatial averaging of  $T$  over a distance equal to the radius of investigation of the injection operation for each point of the aquifer. This averaging process allows the use of relevant effective  $T$  values for given operating conditions. Desbarats (1992) showed that in the case of radial flow to a well, a good estimate of the effective  $T$  is obtained using a weighted geometric average where the weight is taken equal to the inverse of the squared distance from the well. The details of this procedure are given in Appendix A. The radius of investigation is taken as the distance from the well at which the build-up at the end of injection is equal to 1% of the build-up at the well (Bresciani et al., 2020).

### 2.2.3. Injection duration

Injection duration refers to the time over which water will be injected for the purpose of ASR. This will depend on the well efficiency, the volume of available water for injection, and local ASR needs. If we assume an ideal condition of continuous well operation without operational failure, the maximum  $t_{inj}$  becomes a function of source water availability. Potential sources of available water for injection include surface water (reservoir, pond, lake, river, etc.), adjacent aquifers, treated wastewater, or storm water. When the source is rainfall stored in a reservoir, lake, or pond,  $t_{inj}$  depends on precipitation as well as surface storage potential. When river water is the source,  $t_{inj}$  may depend on the time during which discharge exceeds the environmental and other agricultural needs. Thus,  $t_{inj}$  will be highly variable depending on the site context and objectives.

### 2.2.4. Storativity

Storativity ( $S$ ) is another key aquifer parameter that is required for injection capacity estimation. Unlike transmissivity ( $T$ ), storativity cannot be obtained from specific capacity tests. Furthermore, hydraulic head data from observation wells are required for a reliable estimation of storativity because an additional head loss at a pumping well makes it difficult to accurately estimate storativity (Butler, 1990; Fetter, 2001). Thus, storativity values are typically much fewer than transmissivity values. Luckily,  $S$  generally has a much smaller impact on injection capacity than  $T$  (Shandilya et al., 2022). Hence, the spatial variability of  $S$  within a same aquifer formation is not likely to significantly impact the results. Consequently, we opt for simply using the arithmetic mean of four and two  $S$  values of confined and unconfined portion, respectively, of Buffalo aquifer. This approximation is in accordance with the study by Neuman (1982) that showed that  $S$  values tend to be normally distributed in an aquifer and that an arithmetic average can be used for practical purposes.

### 2.2.5. Well radius

Well radius refers to the radius of wellbore pipe. Generally, well radius ( $r_w$ ) is on the order of tens of centimeters and varies depending on the application and site context.  $r_w$  for an injection capacity estimation can be determined based on the radius of operational wells and their respective use in the nearby areas. Our recent study showed that well radius has little influence on the injection capacity value compared to other parameters (Shandilya et al., 2022). Therefore, we use a constant value of  $r_w$  in this study.

## 2.3. Mapping procedure

In this section, we briefly discuss how to compile the database of the parameters and how we combine them to calculate the aquifer-scale injection capacity. We use the raster maps for spatially variable parameters such as  $D$ ,  $ATE$ ,  $K$ , aquifer thickness, etc., and constant values for the remaining parameters ( $\nu_i$ ,  $\rho_w$ , etc.). Then we use the “raster calculator” tool in ArcGIS to calculate  $h_{fp}$ ,  $h_{ap}$ , and  $h_{max}$ . For producing aquifer-scale map of  $h_0$ , we use the “kriging” interpolator in ArcGIS. Finally, raster subtraction of  $h_{max}$  and  $h_0$  gives  $\Delta h_{max}$ . Similarly, we use the “kriging” interpolator for producing spatial map of  $K$ . For transmissivity estimation and averaging process, we use combination of raster calculator and a geostatistical analyst tool. For the rest three parameters ( $t_{inj}$ ,  $S$  and  $r_w$ ) of Eq. (5), we use constant values (details in Section 4.3). The injection capacity is calculated with a Python script due to the exponential integral function in Eq. (5), which is not available in the raster calculator tool of ArcGIS. In Python, this function is available in the SciPy package (Jones et al., 2001). After running the Python script, we obtain a raster file of aquifer-scale injection capacity. We then process the raster file in

ArcGIS for visual presentation.

### 3. Study area description

In this section, we introduce two study areas where the proposed methodology was applied to produce aquifer-scale, injection-capacity maps. We discuss the geographic locations, physiography of the study areas, and potential needs for ASR. Further, we describe the hydrogeologic setting of the target aquifers such as aquifer extent, thickness, material properties (composition and grain size), conditions of confinement, and genesis.

#### 3.1. Buffalo aquifer, Clay County

Clay County, which lies in northwestern Minnesota (Fig. 4), is largely an agriculture-dominated area with small towns. The Buffalo aquifer (Fig. 4a) has been the most heavily utilized aquifer in this County (Berg, 2018). In addition to withdrawals for rural domestic use and irrigation purposes, the aquifer was extensively used by the city of Moorhead (the largest city in northwest Minnesota) for municipal water supply (Berg, 2018) until shortages necessitated a switch to using more Red River water. The current heavy usage and projected population growth in Clay County have raised concerns about the long-term sustainability of the aquifer, and MAR may be a potential solution to ensure the sustainability of the Buffalo aquifer, especially during years of low water flow in the Red River.

The Buffalo aquifer is an elongate, narrow, north-south trending aquifer that extends along much of the western part of Clay County, and south into neighboring Wilkin County. Our study focused on the aquifer within Clay County between the Red River to the west and a branch of the Buffalo River to the east (Fig. 4). The Buffalo aquifer is a partially confined, sand and gravel aquifer of glacial origin with a well-known extent (Fig. B.1, Appendix B), and the total area of the aquifer in Clay County is nearly 100 km<sup>2</sup>. It ranges in thickness from a few meters at the outer edges to about 60 meters locally along the north-south centerline (Appendix B). We used the

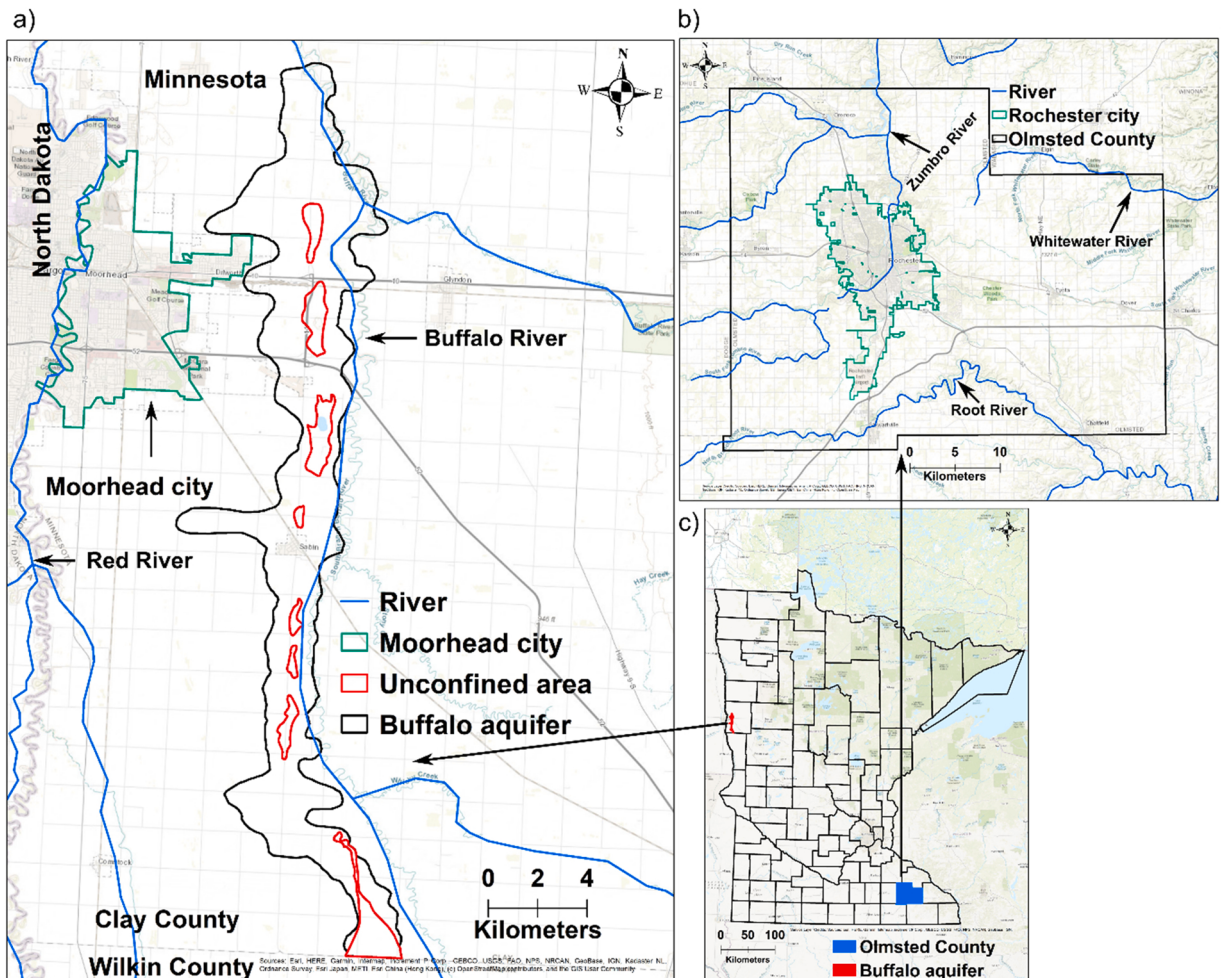


Fig. 4. Maps showing the locations of the study sites (a) Buffalo aquifer, Clay County, and (b) Olmsted County in (c) Minnesota, USA.

maps and geographic information system (GIS) coverages in Bauer (2014) to provide the geologic characteristics of the Buffalo aquifer necessary for the estimation of the injection capacity.

Overall, the aquifer is a heterogeneous mixture of material ranging in size from clay to gravel (Schoenberg, 1998; Wolf, 1981). The aquifer is generally finer-grained along its east and west margins than along its north-south axis. It grades from silty fine- to medium-grained sand near the axis to very fine-grained sand, silt, and clay along the margins (Wolf, 1981). The coarsest material, locally including gravel, is generally in the deepest parts of the aquifer along the axis. The recharge to the Buffalo aquifer may be largely from Wilkin County to the south through a large unconfined area (Wolf, 1981) that represents the proglacial fan. The aquifer is also locally recharged in Clay County through an unconfined portion of the Buffalo aquifer and via leakage through the overlying confining unit (Wolf, 1981). For more information on the physiography of Clay County and aquifer genesis and its interlayered zonation, we refer to Jennings et al. (2021), where a detailed explanation is provided.

### 3.2. Jordan aquifer, Olmsted Count

Olmsted County is in southeastern Minnesota (Fig. 4). It has a gently undulating topography in uplands and is steeper along streams. Most of the land is used for agriculture, with the exception of the city of Rochester (Fig. 4b), the largest city in the county which houses a large medical campus, the Mayo Clinic. The county obtains 100% of its water from groundwater and Rochester is the county's largest consumer of water by a large margin. The Jordan aquifer is the primary source, although many wells are also constructed to extract water from other bedrock units (Delin, 1991; Runkel, 1996). Rochester is rapidly growing compared to other metropolitan areas in the Midwest and is in fact one of the fastest-growing cities in the region. Because of this rapid growth and the exclusive dependence on groundwater, it is important to study the potential of ASR in this region for ensuring the long-term sustainability of its aquifers, especially the heavily used Jordan aquifer.

The Jordan aquifer and other bedrock hydrogeological units in Olmsted County extend across much of southeastern Minnesota (Runkel et al., 2003; Steenberg et al., 2020). The deeper, bedrock geological units in the study area were deposited in early Paleozoic time in a shallow sea. The bedrock layers most important to this study are the fine- to coarse-grained Jordan Sandstone and the overlying Prairie du Chien Group (Fig. B.2, Appendix B). The Prairie du Chien Group includes two formations, the Oneota Dolomite, and the overlying Shakopee Formation (Fig. B.2, Appendix B), both consisting largely of dolostone. The Shakopee and the upper part of

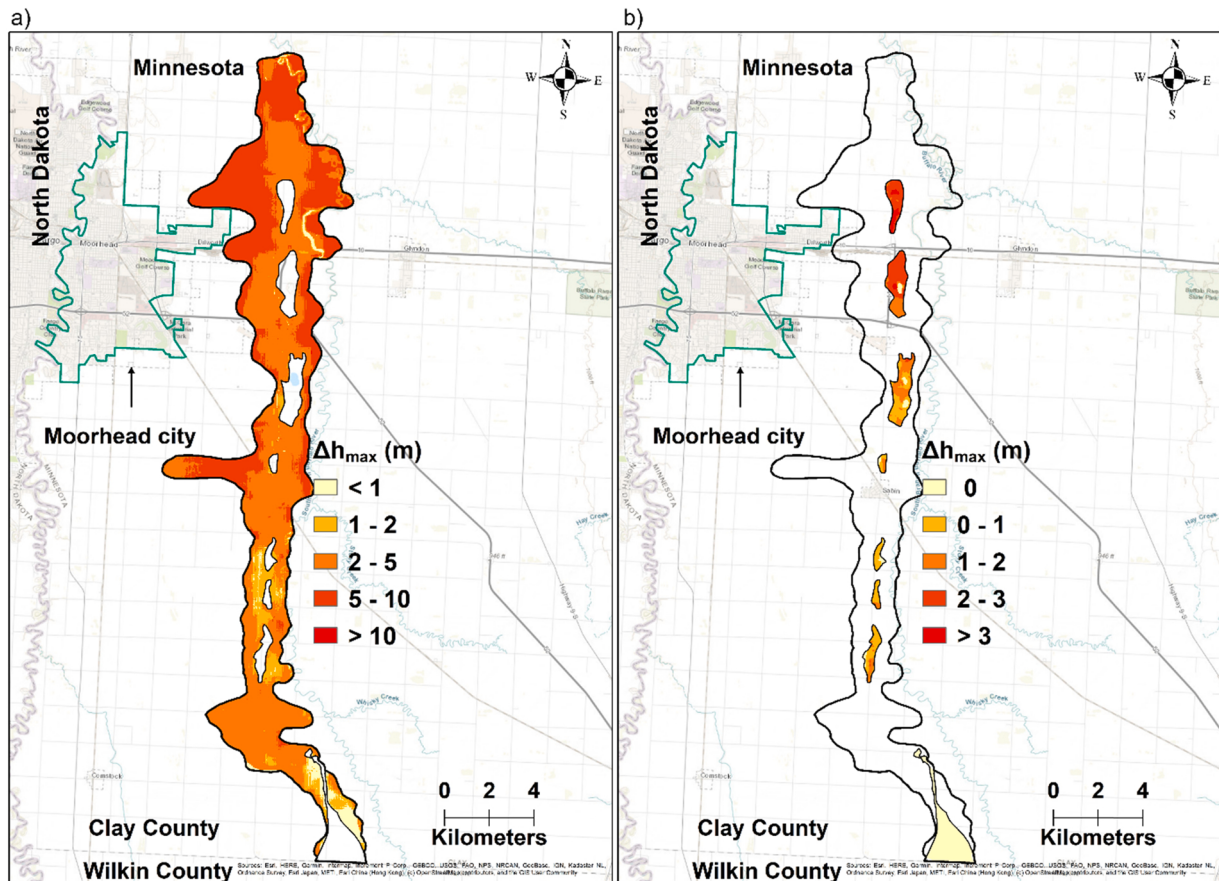


Fig. 5. Maps showing allowable hydraulic head change for (a) the confined portion, and (b) the unconfined portion of the Buffalo aquifer.

Oneota Dolomite are classified as an aquifer in the region. The lower approximately two-thirds of the Oneota Dolomite is an aquitard confining the underlying Jordan aquifer. We used the maps and related GIS coverages in Steenberg et al. (2020) to provide the geologic characteristics of the Jordan aquifer necessary for our injection capacity estimation.

In Olmsted County, the Jordan aquifer is regarded as having more or less homogeneous hydraulic properties (Balaban, 1988; Delin, 1991). However, substantial variation in municipal well productivity has been recognized and was attributed by Runkel (1996) to varying thickness of the coarse clastic sandstone in the aquifer. Areas where the aquifer has a relatively thick section of coarse clastic sandstone were shown to be more productive than areas where such strata are thinner. For detailed information on the Jordan aquifer in Olmsted County, we refer to Jennings et al. (2021).

#### 4. Results and discussion

In this section, we apply the proposed methodology to produce aquifer-scale  $\Delta h_{\max}$  (Section 4.1) and  $T$  (Section 4.2) maps for both study sites. We then discuss the other three parameters ( $t_{inj}$ ,  $S$  and  $r_w$ ) in Section 4.3, and combine them with  $\Delta h_{\max}$  and  $T$  maps to produce injection capacity maps in Section 4.4. We discuss the relative importance of the input parameters in determining the obtained injection capacity maps and explain what caused high or low injection capacity regions. We then estimate the required number of wells to inject the volume of water equal to one month of domestic water demand. Finally, we discuss the advantages and limitations of the proposed methodology in Section 4.5.

##### 4.1. Maximum allowable hydraulic head change

In this subsection, we present the results of  $\Delta h_{\max}$  maps for both sites. All the supplementary information related to the generation of  $\Delta h_{\max}$  is given in Appendix C.  $\Delta h_{\max}$  map of confined portion of Buffalo aquifer (Fig. 5a) shows that values are high in the northern portion and along the west and east margins because of larger  $h_{fp}$  (Fig. C.1, Appendix C). The larger overburden thickness and lower groundwater elevation (Fig. C.2, Appendix C) leads to a large headspace for injection. Low  $\Delta h_{\max}$  values are mostly from the confined-unconfined transition zone areas of the aquifer, where  $h_{\max}$  values are comparatively lower due to the low values of  $h_{fp}$ . In the southern portion,  $\Delta h_{\max}$  is comparatively low even though  $h_{\max}$  is high because the groundwater elevation is relatively high. Overall,  $\Delta h_{\max}$  is small (2–5 m) in the majority of the confined portion. The mean value of  $\Delta h_{\max}$  are 4.22 m and the coefficient of variation (standard deviation over mean) is 0.4 (Table 2).

For  $\Delta h_{\max}$  calculation of the unconfined portion of Buffalo aquifer, we use 2.5 m as a safety limit to avoid saturating the soil root zone. Overall,  $\Delta h_{\max}$  is small (Fig. 5b), indicating that the groundwater elevation is close to the land surface. We confirm that the groundwater elevation is in general close to the land surface by plotting the depth-to-static-groundwater map (Fig. C.3, Appendix C). In the southern part of the unconfined aquifer,  $\Delta h_{\max}$  is small because the groundwater elevation is close to the land surface. In the middle part,  $\Delta h_{\max}$  is also marginal and may not be considered an ideal location for injection. In the north part, moderate values of  $\Delta h_{\max}$  are obtained, where 2–3 m of headspace can be used for injection due to the greater depth to the groundwater table (3–5 m). The mean  $\Delta h_{\max}$  value is 1.0 m and the standard deviation is 1.03 m (Table 2).

For the Jordan aquifer in Olmsted County,  $\Delta h_{\max}$  is also calculated at 85% of  $h_{fp}$ , and we only present key results and refer to Appendix C (Fig. C.4 and Fig. C.5) for detailed information. The obtained  $\Delta h_{\max}$  map shows that more than 75 m of head change is allowed in about half of the County. The mean value of  $\Delta h_{\max}$  is 77.8 m and the coefficient of variation is 0.38 (Table 2). The regions corresponding to  $\Delta h_{\max} > 75$  m mostly match those where overburden thickness is large (> 150 m) (Fig. 6a and Fig. 6b). Most of the

**Table 2**

Comparison of key estimated variables at the two study sites.

Statistical comparison			
	Buffalo aquifer	Confined	Jordan aquifer Olmsted County
Mean value	3457.0	853.39	107.40
Median value	843.89	270.41	109.95
Standard deviation	5246.28	1775.82	13.83
Coefficient of variation	1.52	2.08	0.13
Allowable hydraulic head change (m)			
Mean value	1.0	4.22	77.87
Median value	0.75	4.13	78.51
Standard deviation	1.03	1.69	29.21
Coefficient of variation	1.02	0.4	0.38
Injection capacity ( $10^6 \text{ m}^3$ )			
Mean value	0.1	0.06	0.14
Median value	0.01	0.02	0.15
Standard deviation	0.17	0.12	0.06
Coefficient of variation	1.69	1.99	0.4
90 <sup>th</sup> percentile value	0.39	0.16	0.22
99 <sup>th</sup> percentile value	0.7	0.56	0.26

remainder of the county has  $\Delta h_{\max}$  between 25–75 m. Regions with  $\Delta h_{\max} < 25$  m are in the vicinity of river channels. Throughout Olmsted County, a close correlation exists between the overburden thickness and  $\Delta h_{\max}$  maps (Fig. 6). This implies that the variability in  $\Delta h_{\max}$  is largely controlled by the overburden thickness, and the variability of groundwater level is relatively small.

#### 4.2. Transmissivity

Here, we present and discuss transmissivity ( $T$ ) maps of both sites. Note that because the Buffalo aquifer has unconfined as well as confined portions, we used the two different criteria for estimating  $T$ , as outlined in Section 2.2.2.

The  $T$  map shows a high variability across the aquifer (Fig. 7). The coefficient of variation of  $T$  for the confined portion is 2.08 (Table 2) indicating that the standard deviation is more than twice the mean  $T$ . In the northern portion of the aquifer, the variability in  $T$  is comparatively larger in both confined and unconfined aquifers due to larger variability in both  $K$  (Fig. D.1, Appendix D) and thickness (Fig. D.2, Appendix D). In the southern portion, variability is comparatively smaller. Smaller variation in aquifer thickness and saturated thickness may be one of the possible reasons. However, the lower variability in  $T$  in the southern portion is also likely due to the low data density of  $K$ . Lower values ( $< 100 \text{ m}^2/\text{d}$ ) are mostly from the west and east margins whereas higher values ( $> 3000 \text{ m}^2/\text{d}$ ) are mostly along the north-south axis. The unconfined parts of the aquifer mostly show moderate to high  $T$  values because the saturated thickness is relatively large, and aquifer materials are coarse grained.

The  $T$  map (Fig. 8) of the Jordan aquifer in Olmsted County is mainly controlled by the variation in  $K$  of the aquifer. More detailed information regarding  $K$  and aquifer thickness maps can be found in Appendix D. In the majority of Olmsted County, the Jordan aquifer thickness is approximately 30 m (100 feet) (Fig. D.3, Appendix D). Thus, the aquifer thickness contributes little to the  $T$  variability.  $T$  varies approximately by one order of magnitude with the coefficient of variation of 0.13 (Table 2), which is significantly smaller than the Buffalo aquifer. In the majority of the County, the  $T$  values are between 60 and 150  $\text{m}^2/\text{d}$ .

#### 4.3. Injection duration, storativity, and well radius

In this subsection, we discuss the other three input parameters:  $t_{\text{inj}}$ ,  $S$ , and  $r_w$ . For this study, we select one month of  $t_{\text{inj}}$  for both sites. The reason behind selecting this injection duration for both areas is that source water will be available for injection in both sites at least for one month. For the Buffalo aquifer, we treated the  $S$  values of confined and unconfined portions separately. The arithmetic average of  $S$  values from four locations of the confined portion of the Buffalo aquifer is 0.003, whereas the unconfined portion has the arithmetic average of 0.17 from two locations. For Olmsted County, we use the model calibrated  $S$  value of  $1 \times 10^{-4}$  from Christianson (2018).

Wells used for specific capacity tests in both areas have  $r_w$  in the range of 5–50 cm. For ASR study purposes,  $r_w$  in the range of 10–20 cm is reported from Australia and USA (Dudding et al., 2006; Gibson et al., 2018). We use a constant  $r_w$  value of 15 cm for both study areas.

#### 4.4. Injection capacity

We produced injection capacity maps (Fig. 9) using the five input parameters presented in the previous subsections. The estimated

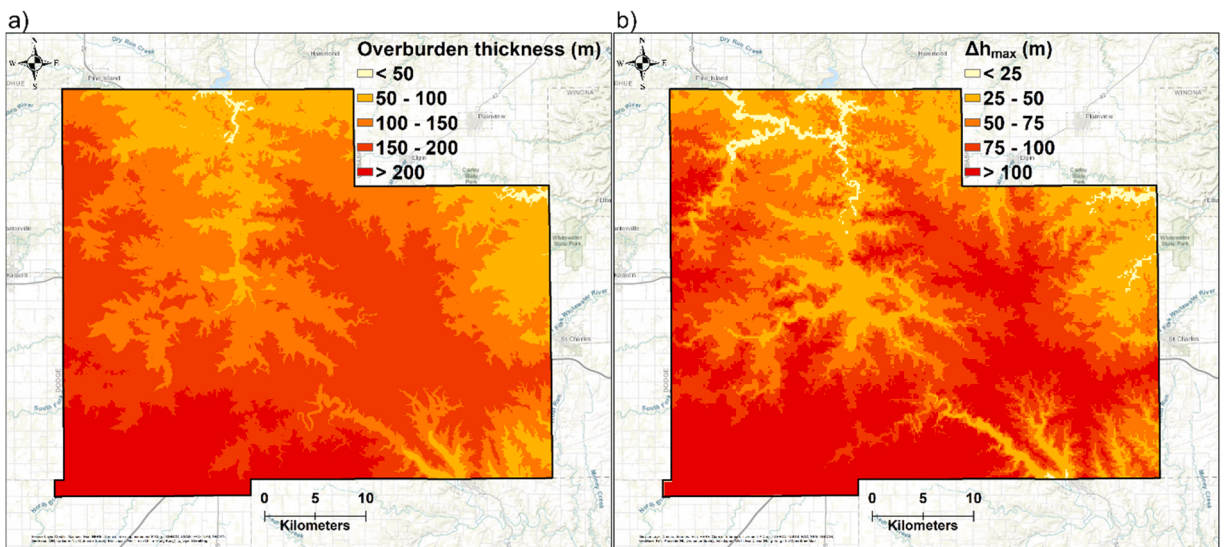


**Fig. 6.** Maps showing (a) overburden thickness, and (b) allowable hydraulic head change above the initial groundwater elevation of the Jordan aquifer in Olmsted County.

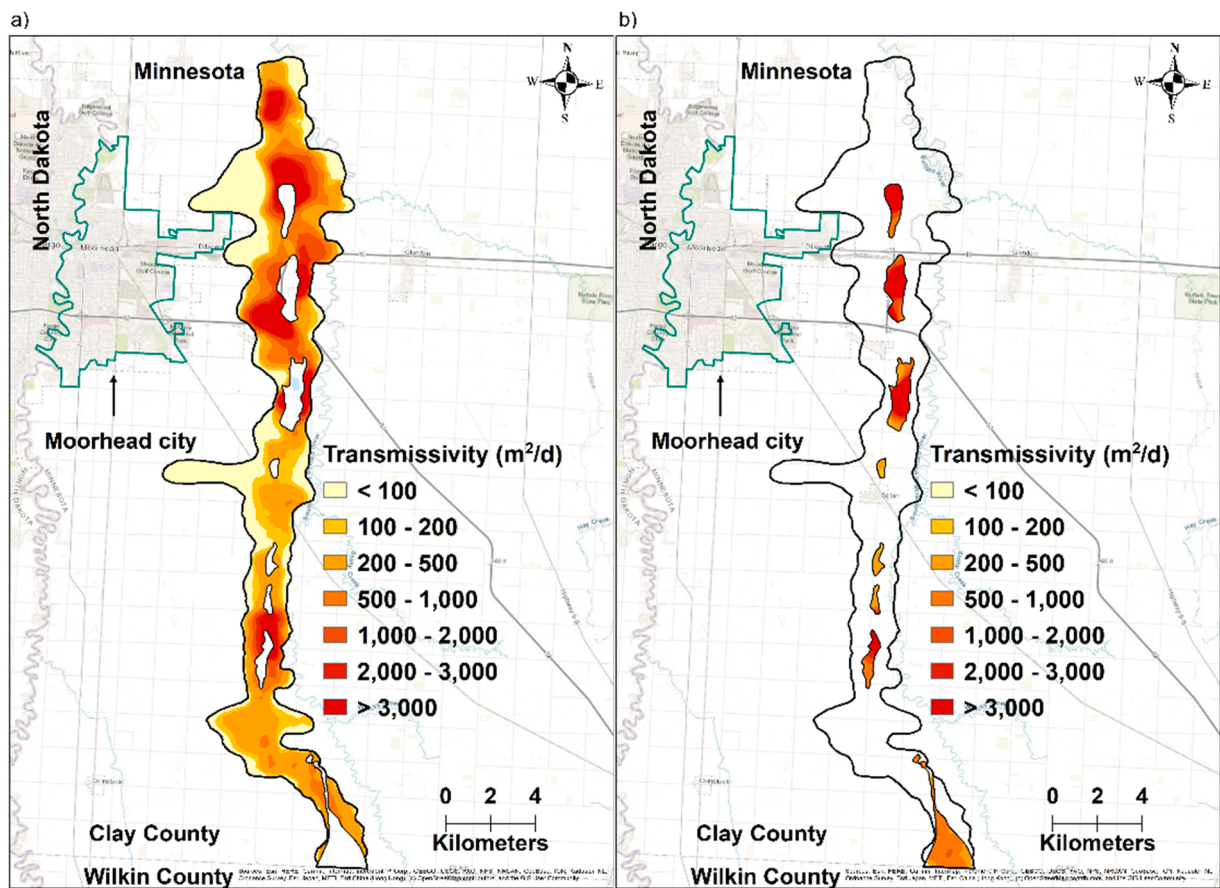


Fig. 7. Transmissivity maps of (a) the confined and (b) unconfined portions of the Buffalo aquifer.

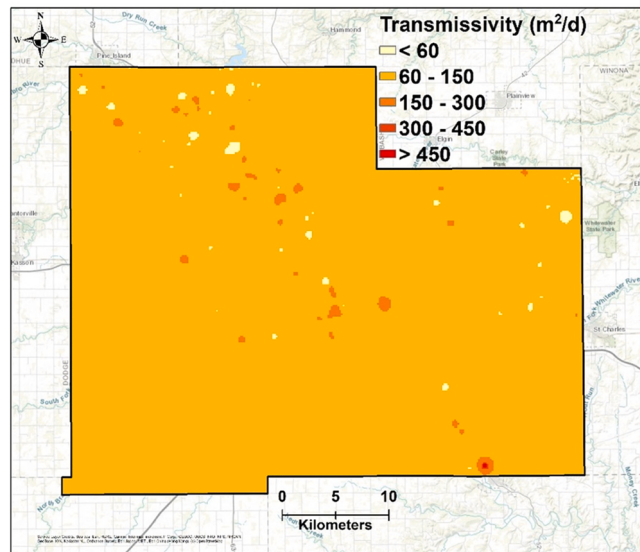


Fig. 8. Transmissivity map of the Jordan aquifer in Olmsted County.

injection capacity values vary over a wide range in the Buffalo aquifer (Fig. 9a). The variation in the injection capacity is due to the variability in both  $T$  and  $\Delta h_{\max}$  values across the aquifer. The  $\Delta h_{\max}$  values vary significantly across the aquifer, ranging from negligible up to 13 m. The overall injection capacity map is largely dominated by the  $T$  map because the variability of  $T$  values are larger compared to  $\Delta h_{\max}$  values. We observe negligible injection capacity values in the southernmost and westernmost portions of the aquifer. The  $\Delta h_{\max}$  values are negligible due to the shallow groundwater depths in the southernmost portion, and  $T$  values are very small along the westernmost portion. Higher injection capacity is present mostly in the central region of the northern area, where  $T$  is large and  $\Delta h_{\max}$  is in the mid-range. The area with the highest injection capacity value is where  $T$  is highest.

There is also significant spatial variability in the injection capacity for the Jordan aquifer in Olmsted County (Fig. 9b). A comparison with the  $\Delta h_{\max}$  map (Fig. 6b) shows that the estimated injection capacity values across most of Olmsted County are controlled by the  $\Delta h_{\max}$ , which is controlled by the overburden thickness (Fig. 6a). This is because the variability of  $\Delta h_{\max}$  is much larger than the  $T$  variability at this site. Areas near the Zumbro River in the north, the Whitewater River in the east, and the Root River in the south show lower injection capacity. The lower  $\Delta h_{\max}$  in these areas cause the lower injection capacity. In the south and southwest parts of the county, injection capacity is higher. These are the regions where the aquifer has higher  $\Delta h_{\max}$  and mid-range  $T$ . Overall, we observe large areas of the county having mid-range injection capacity values, whereas lower injection capacity is only from localized areas in the north and east.

The injection capacity of the two study areas show different characteristics. First, the injection capacity of the Buffalo aquifer has a larger variability as compared to the Jordan aquifer (Table 2). Both  $T$  and  $\Delta h_{\max}$  vary widely in the Buffalo aquifer, but  $T$  is relatively homogeneous in the Jordan aquifer. The 99<sup>th</sup> percentile value of injection capacity is significantly higher in both confined and unconfined portions of the Buffalo aquifer than in the Jordan aquifer whereas the 90<sup>th</sup> percentile value of injection capacity in the confined portion of the Buffalo aquifer is lower than in the Jordan aquifer. This indicates that some local areas in the Buffalo aquifer have very high injection capacity, which is due to high  $T$ . A comparison of the median injection capacity values between the two study sites shows that the median value of the Buffalo aquifer is an order of magnitude smaller, even though the maximum injection capacity value of the Buffalo aquifer is significantly higher than that of the Jordan aquifer. This is due to the large overburden thickness in the Jordan aquifer and significant variability in both  $T$  and  $\Delta h_{\max}$  in the Buffalo aquifer. In the confined portion of the Buffalo aquifer, the median value is close to 2.9% of the 99<sup>th</sup> percentile value, which indicates that most of the area has injection capacity values significantly smaller than the 99<sup>th</sup> percentile value.

We now discuss the relevance of the estimated injection capacity values for serving the Moorhead and Rochester populations. To determine whether the estimated injection capacity values are sufficient to meet the domestic water use of these cities, we conduct a simple calculation based on the total population of the respective cities, per capita domestic water use, total domestic water use for one month, and 90<sup>th</sup> percentile value of injection capacity (Table 3).

In Table 3, we present the calculations with the 90<sup>th</sup> percentile value of injection capacity at both sites, and the calculations indicate that two wells and four wells are needed to inject the amount of water equivalent to one month of domestic water needs for the cities of Moorhead and Rochester, respectively. If we target areas with higher injection capacity values, fewer wells may be required. Note that

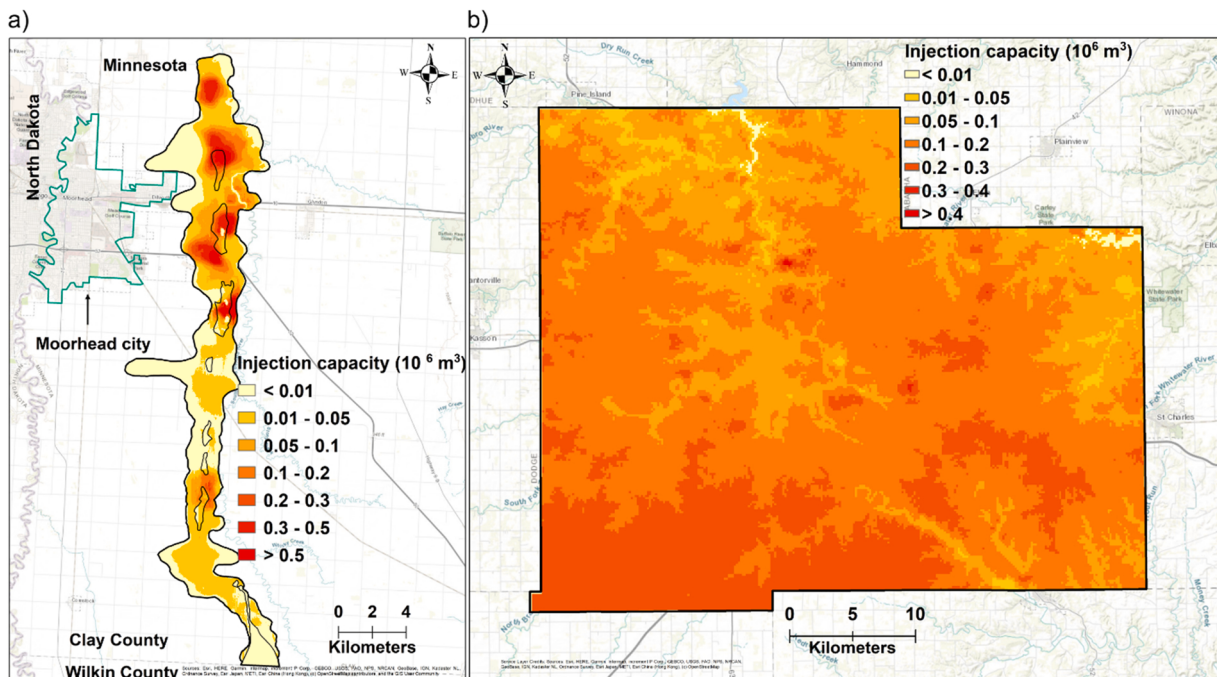


Fig. 9. Injection capacity maps of (a) the Buffalo aquifer in Clay County and (b) the Jordan aquifer in Olmsted County.

**Table 3**

Relevance of injection capacity volume for serving the populations of Moorhead and Rochester with one-month injection duration.

	Moorhead	Rochester
Population as of July 1, 2019	43,652 (U. S. <a href="#">Census Bureau, 2019a</a> )	118,935 (U. S. <a href="#">Census Bureau, 2019b</a> )
Per capita domestic water use of Minnesota	0.22 m <sup>3</sup> ( <a href="#">Dieter et al., 2018</a> )	
Total volume of domestic water use per day in the city	9603 m <sup>3</sup>	26,166 m <sup>3</sup>
90 <sup>th</sup> percentile value of injection capacity	180,761 m <sup>3</sup>	221,320 m <sup>3</sup>
Number of days served for domestic water use by a single well injecting for one month	19 days	8 days
Number of wells required to inject water equivalent to one month of domestic water use	2 wells	4 wells

we did not consider well interference between injection wells. Closely spaced wells may result in reduced injection capacity due to well interference, and thus, more wells may be required to store the target volume.

Another aspect to consider is the risk of causing flowing-well conditions near an injection well (where the hydraulic head is higher than the ground level). For confined aquifers,  $\Delta h_{\max}$  may cause flowing well conditions in the wells that are close to the injection well. To avoid any risk of flowing well conditions,  $h_{\max}$  could be set to the ground level. However, this may be too conservative choice and may lead to a significant reduction in injection capacity. Instead, injection wells could be located at a sufficient distance from existing wells to avoid this potential problem. To check the required distance, we produced a hydraulic head profile at a point in the Buffalo aquifer with 99<sup>th</sup> percentile value of injection capacity. A plot of the head profile at the end of the injection displays a sharp decline in the hydraulic head as the distance increases from the injection well ([Fig. 10](#)). The plot indicates that any well located more than a few meters away from the injection well will not experience flowing-well conditions.

#### 4.5. Advantages and limitations of the proposed method

The methodology proposed in this study has significant advantages over qualitative ASR site suitability estimation methods. Most importantly, it enables a quantitative, physically-based estimation of injection capacity at aquifer-scale. This is the first study that proposes a continuous aquifer-scale mapping methodology for both unconfined and confined aquifers. The produced injection capacity map enables one not only to select the optimal injection well locations but also to estimate the actual amount of water that could be injected in one month. This is another important advantage over studies such as [Dudding et al. \(2006\)](#) where only categorization of the aquifer as zones of a low, medium, or high injection potential is done. While being physically based, the methodology remains simple, thus enabling efficient first-order estimation of injection capacity. Additionally, in case of change in any parameter value (e.g., different injection duration), one can easily reevaluate the injection capacity and efficiently produce an updated aquifer-scale, injection capacity map. However, high quality and high spatial density of key parameters such as transmissivity, overburden thickness and groundwater elevation are important for an accurate estimation of injection capacity. Therefore, the methodology is best suited for areas where good background information is available.

The method is based on the Theis solution so the proposed method inherits the assumptions of the Theis solution mentioned in [Section 2.1](#). Heterogeneity in aquifer properties may cause noticeable differences in the injection capacity. However, the averaging process outlined in [Section 2.2.2](#) should largely alleviate this issue. The applicability of an equation established for a confined aquifer to an unconfined aquifer depends on the ratio of change in saturated thickness to initial saturated thickness ([Bear, 1979](#)). Therefore, as long as  $\Delta h_{\max}$  is small relative to the initial saturated thickness of an unconfined aquifer, this methodology can be safely applied to an unconfined aquifer; otherwise, non-negligible errors may be introduced. If inter-aquifer leakage, partial-penetration or boundary effects are significant, one may need to extend the methodology by using drawdown solutions that consider these effects. The development of a skin layer may cause a significant reduction in injection capacity with the aging of wells, but well-redevelopment measures applied at regular intervals can minimize this effect ([Barrash et al., 2006; Houben, 2015](#)). Thus, it is not an intrinsic aquifer property, and so one may not consider it when evaluating potential sites. Wellbore storage is only significant for large-diameter wells with short pumping times ([Papadopoulos and Cooper, 1967](#)), and thus it only needs to be considered when the injection duration is very short.

## 5. Conclusions

In this study, we developed a new GIS-based methodology that produces injection capacity maps and demonstrated it by using Minnesota's extensive hydrogeologic database for the necessary parameters. We successfully produced injection capacity maps for two aquifers in Minnesota: the Buffalo aquifer in Clay County and the Jordan aquifer in Olmsted County. The results reveal that the selected study areas have large spatial variabilities in the injection capacity. This demonstrates the relevance of producing such maps to guide the siting of injection locations. The Buffalo aquifer shows higher variability in the injection capacity than the Jordan aquifer, which is mainly caused by its larger variability in  $T$ . In contrast, the injection capacity of the Jordan aquifer is governed by the variability of  $\Delta h_{\max}$ . These two case studies show that the variability of injection capacity can be governed by both  $T$  and  $\Delta h_{\max}$ , which are part of the hydrogeologic setting of a site. The importance of  $T$  and  $\Delta h_{\max}$  for injection capacity estimation emphasizes the need for high-quality  $K$ , aquifer thickness, overburden thickness, and groundwater elevation maps.

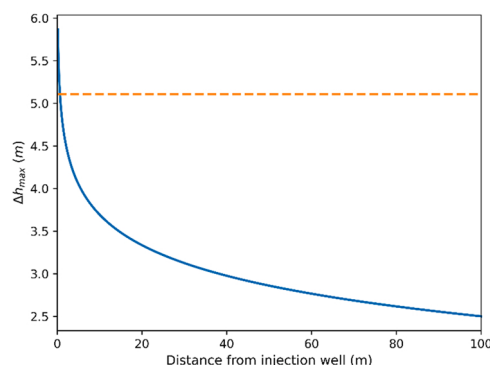


**Fig. 10.** Hydraulic head profile as a function of distance from the injection well. The  $\Delta h_{\max}$  value at injection point is  $\sim 6$  m. The dashed line shows the ground-surface level.

The mapping methodology is based on the Theis solution, which relies on various assumptions. Thus, when applying the methodology, one should be aware of the potential limitations as discussed in Section 4.5. For example, to minimize the effect of aquifer heterogeneity,  $K$  values should ideally be estimated from aquifer pumping tests with a duration close to the target injection duration, or one could perform an averaging procedure as discussed in Section 2.2.2. Considering that no aquitard is perfectly impermeable, an important extension of the proposed methodology would be to account for leakage through a confining unit.

The produced injection capacity maps suggest that the volume of water equivalent to the domestic water use for one month can be injected in both study areas using two and four wells, respectively, with an injection duration of one month. Locally, higher injection capacities may be found, in which case the number of required wells could be reduced. Although more detailed studies are needed to confirm these findings, our study suggests that the hydrogeologic conditions of the Buffalo aquifer and the Jordan aquifers are suitable for the development of ASR projects for domestic use. This study demonstrates the usefulness of the proposed methodology that enables a first-order quantification of well-based injection capacity. By combining with a socio-economic evaluation, the proposed tool will help stakeholders to assess the feasibility of potential ASR sites.

#### CRediT authorship contribution statement

**Raghwendra N. Shandilya:** Software, Formal analysis, Writing - Original Draft, Data Curation, Visualization, Investigation. **Etienne Bresciani:** Conceptualization, Supervision, Methodology, Investigation, Writing - Review & Editing. **Anthony C. Runkel:** Investigation, Data Curation, Visualization, Writing - Original Draft. **Carrie E. Jennings:** Funding acquisition, Writing - Review & Editing. **Seunghak Lee:** Supervision, Funding acquisition, Writing - Review & Editing. **Peter K. Kang:** Conceptualization, Project administration, Supervision, Investigation, Validation, Funding acquisition, Writing - Review & Editing.

#### Declaration of Competing Interest

The authors declare that they have no known competing financial interests or personal relationships that could have appeared to influence the work reported in this paper.

#### Acknowledgments

The authors acknowledge support from the National Research Foundation of Korea (NRF) through the ‘Climate Change Impact Minimizing Technology’ Program funded by the Korean Ministry of Science and ICT (MSIT) (2020M3H5A1080712), the Korea Research Fellowship program funded by the Ministry of Science and ICT through the National Research Foundation of Korea (grant 2016H1D3A1908042), the Korea Environment Industry & Technology Institute (KEITI) through the Subsurface Environment Management (SEM) Project (2018002440006) funded by the Korea Ministry of Environment (MOE), and the Minnesota Environment and Natural Resources Trust Fund as recommended by the Legislative-Citizen Commission on Minnesota Resources (LCCMR).

#### Appendix A. Supporting information

Supplementary data associated with this article can be found in the online version at doi:10.1016/j.ejrh.2022.101048.

## References

- Aeschbach-Hertig, W., Gleeson, T., 2012. Regional strategies for the accelerating global problem of groundwater depletion. *Nat. Geosci.* 5 (12), 853–861. <https://doi.org/10.1038/NGE01617>.
- Ahmed, S., De Marsily, G., 1987. Comparison of geostatistical methods for estimating transmissivity using data on transmissivity and specific capacity. *Water Resour. Res.* 23 (9), 1717–1737. <https://doi.org/10.1029/WR023i009p01717>.
- Alazard, M., Leduc, C., Travi, Y., Boulet, G., Salem, A.B., 2015. Estimating evaporation in semi-arid areas facing data scarcity: example of the El Haouareb dam (Merguellil catchment, Central Tunisia). *J. Hydrol.: Reg. Stud.* 3, 265–284. <https://doi.org/10.1016/j.ejrh.2014.11.007>.
- Balaban, N.H., 1988. C-03 Geologic atlas of Olmsted County, Minnesota. Minnesota Geological Survey, St. Paul, Minnesota. Retrieved Univ. Minn. Digit. Conserv. (<https://hdl.handle.net/11299/58436>).
- Barrash, W., Clemo, T., Fox, J.J., Johnson, T.C., 2006. Field, laboratory, and modeling investigation of the skin effect at wells with slotted casing, Boise Hydrogeophysical Research Site. *J. Hydrol.* 326 (1–4), 181–198. <https://doi.org/10.1016/j.jhydrol.2005.10.029>.
- Bauer, E.J., 2014. Data base map. Minnesota Geological Survey, St. Paul, Minnesota. Retrieved from the University of Minnesota Digital Conservancy, (<http://hdl.handle.net/11299/163570>).
- Bear, J., 1979. *Hydraulics of groundwater*. McGraw-Hill, New York, p. 952.
- Berg, J.A., 2018. Geologic atlas of Clay County, Minnesota. Minnesota Department of Natural Resources, St. Paul, Minnesota. Retrieved Univ. Minn. Digit. Conserv. (<https://hdl.handle.net/11299/163570>).
- Bloetscher, F., Sham, C.H., Danko, J.J., Ratnick, S., 2014. Lessons learned from aquifer storage and recovery (ASR) systems in the United States. *J. Water Resour. Prot.* 6 (17), 1603–1629. <https://doi.org/10.4236/jwarp.2014.617146>.
- Bouwer, H., 2002. Artificial recharge of groundwater hydrogeology and engineering. *Hydrogeol. J.* 10 (1), 121–142. <https://doi.org/10.1007/s10040-001-0182-4>.
- Bradbury, K.R., Rothschild, E.R., 1985. A computerized technique for estimating the hydraulic conductivity of aquifers from specific capacity data. *Groundwater* 23 (2), 240–246. <https://doi.org/10.1111/j.1745-6584.1985.tb02798.x>.
- Bresciani, E., Shandilya, R.N., Kang, P.K., Lee, S., 2020. Well radius of influence and radius of investigation: what exactly are they and how to estimate them? *J. Hydrol.* 583. <https://doi.org/10.1016/j.jhydrol.2020.124646>.
- Brown, C.J., Weiss, R., Verrastro, R., Schubert, S., 2005. Development of an aquifer, storage and recovery (ASR) site selection suitability index in support of the comprehensive everglades restoration project. *J. Environ. Hydrol.* 13 (20), 13.
- Butler, J.J., 1990. The role of pumping tests in site characterization: some theoretical considerations. *Groundwater* 28 (3), 394–402. <https://doi.org/10.1111/j.1745-6584.1990.tb02269.x>.
- Christianson, E., 2018. 0. Rochester Groundwater Model Version 2. Barr Engineering company, Minneapolis, Minnesota.
- Collins, M., Knutti, R., Arblaster, J., Dufresne, J.-L., Fichefet, T., Friedlingstein, P., Gao, X., Gutowski, W.J., Johns, T., Krinner, G., Shongwe, M., Tebaldi, C., Weaver, A.J., Wehner, M., 2013. Long-term climate change: projections, commitments and irreversibility. In: Stocker, T.F., et al. (Eds.), *Climate Change 2013-The Physical Science Basis: Contribution of Working Group I to the Fifth Assessment Report of the Intergovernmental Panel on Climate Change*. Cambridge University Press, New York, pp. 1029–1136.
- Craig, I., Green, A., Scobie, M., Schmidt, E., 2005. Controlling evaporation loss from water storages. National Center for Engineering in Agriculture, Toowoomba. (<https://core.ac.uk/download/pdf/11036431.pdf>).
- Delin, G.N., 1991. Hydrogeology and simulation of ground-water flow in the Rochester area, southeastern Minnesota, 1987–88. U. S. Geological Survey, St. Paul, Minnesota.
- Desbarats, A.J., 1992. Spatial averaging of transmissivity in heterogeneous fields with flow toward a well. *Water Resour. Res.* 28 (3), 757–767. <https://doi.org/10.1029/91WR03099>.
- Dieter, C.A., Maupin, M.A., Caldwell, R.R., Harris, M.A., Ivahnenko, T.I., Lovelace, J.K., Barber, N.L., Linsey, K.S., 2018. Estimated use of water in the United States in 2015. U.S. Geological Survey Circular, Reston, Virginia, p. 1441. <https://doi.org/10.3133/circ1441>.
- Dillon, P., 2005. Future management of aquifer recharge. *Hydrogeol. J.* 13 (1), 313–316. <https://doi.org/10.1007/s10040-004-0413-6>.
- Dillon, P., Stuyfzand, P., Grischek, T., Lluria, M., Pyne, R.D.G., Jain, R.C., Bear, J., Schwarz, J., Wang, W., Fernandez, E., Stefan, C., Pettenati, M., Van Der Gun, J., Sprenger, C., Massmann, G., Scanlon, B.R., Xanke, X., Jokela, P., Zheng, Y., Rossetto, R., Shamrukh, M., Pavelic, P., Murray, E., Ross, A., Bonilla Valverde, J.P., Nava, A.P., Ansems, N., Posavec, K., Ha, K., Martin, R., Sapiro, M., 2019. Sixty years of global progress in managed aquifer recharge. *Hydrogeol. J.* 27, 1–30. <https://doi.org/10.1007/s10040-018-1841-z>.
- Dudding, M., Evans, R., Dillon, P., Molloy, R., 2006. Developing Aquifer Storage and Recovery (ASR) opportunities in Melbourne. Report on broad scale map of ASR potential for Melbourne. Victorian Smart Water Fund, Malvern, Australia. URL: ([https://waterportal.com.au/swf/images/swf-files/1145\\_developing-aquifer-storage-amp-recovery-opportunities-in-greater-melbourne\\_mapping-report.pdf](https://waterportal.com.au/swf/images/swf-files/1145_developing-aquifer-storage-amp-recovery-opportunities-in-greater-melbourne_mapping-report.pdf)).
- Famiglietti, J.S., 2014. The global groundwater crisis. *Nat. Clim. Change* 4 (11), 945. <https://doi.org/10.1038/nclimate2425>.
- Famiglietti, J.S., Rodell, M., 2013. Water in the balance. *Science* 340 (6138), 1300–1301. <https://doi.org/10.1126/science.1236460>.
- Fan, J., McConkey, B., Wang, H., Janzen, H., 2016. Root distribution by depth for temperate agricultural crops. *Field Crops Res.* 189, 68–74. <https://doi.org/10.1016/j.fcr.2016.02.013>.
- Fetter, C.W., 2001. *Applied hydrogeology*. Prentice Hall, Upper Saddle River, NJ, p. 598.
- Gibson, M.T., Campana, M.E., Nazy, D., 2018. Estimating aquifer storage and recovery (ASR) regional and local suitability: a case study in Washington State, USA. *Hydrology* 5 (1), 7. <https://doi.org/10.3390/hydrology5010007>.
- Gleeson, T., VanderSteen, J., Sophocleous, M.A., Taniguchi, M., Alley, W.M., Allen, D.M., Zhou, Y., 2010. Groundwater sustainability strategies. *Nat. Geosci.* 3 (6), 378. <https://doi.org/10.1038/ngeo881>.
- Grönwall, J., Danert, K., 2020. Regarding groundwater and drinking water access through a human rights lens: Self-Supply as a norm. *Water* 12 (2), 419. <https://doi.org/10.3390/w12020419>.
- Hodgkin, T., 2004. Aquifer storage capacities of the Adelaide region. Department of Water, Land and Biodiversity Conservation, Adelaide. URL: ([https://www.waterconnect.sa.gov.au/Content/Publications/DEW/dwlbc\\_report\\_2004\\_47.pdf](https://www.waterconnect.sa.gov.au/Content/Publications/DEW/dwlbc_report_2004_47.pdf)).
- Houben, G.J., 2015. Hydraulics of water wells—head losses of individual components. *Hydrogeol. J.* 23 (8), 1659–1675. <https://doi.org/10.1007/s10040-015-1313-7>.
- Jennings, C.E., Billotta, J.P., Arnold, W., Bohman, B., Bresciani, E., Gassman, P., Kang, P.K., Kirby, E., Kirk, J., Lee, S., Levers, L., Runkel, A.C., Shandilya, R.N., Valcu-Lisman, A., Xiang, G., Yoon, S., 2021. Banking Groundwater—A study examining aquifer storage and recovery for groundwater sustainability in Minnesota. University of Minnesota and Freshwater. Retrieved Univ. Minn. Digit. Conserv. (<https://hdl.handle.net/11299/218325>).
- Jones, E., Oliphant, T., Peterson, P., et al., 2001. *SciPy: Open Source Sci. tools Python*.
- Kang, P.K., Bresciani, E., An, S., Lee, S., 2019. Potential impact of pore-scale incomplete mixing on biodegradation in aquifers: from batch experiment to field-scale modeling. *Adv. Water Resour.* 123, 1–11. <https://doi.org/10.1016/j.advwatres.2018.10.026>.
- Khan, S., Mushtaq, S., Hanjra, M.A., Schaeffer, J., 2008. Estimating potential costs and gains from an aquifer storage and recovery program in Australia. *Agric. Water Manag.* 95 (4), 477–488. <https://doi.org/10.1016/j.agwat.2007.12.002>.
- Kim, H., Yang, S., Rao, S.R., Narayanan, S., Kapustin, E.A., Furukawa, H., Umans, A.S., Yaghi, O.M., Wang, E.N., 2017. Water harvesting from air with metal-organic frameworks powered by natural sunlight. *Science* 356 (6336), 430–434. <https://doi.org/10.1126/science.aam8743>.
- Levandowski, W., Herrmann, R.B., Briggs, R., Boyd, O., Gold, R., 2018. An updated stress map of the continental United States reveals heterogeneous intraplate stress. *Nat. Geosci.* 11 (6), 433–437. <https://doi.org/10.1038/s41561-018-0120-x>.
- Mailhot, A., Talbot, G., Ricard, S., Turcotte, R., Guinard, K., 2018. Assessing the potential impacts of dam operation on daily flow at ungauged river reaches. *J. Hydrol.: Reg. Stud.* 18, 156–167. <https://doi.org/10.1016/j.ejrh.2018.06.006>.

- Maliva, R.G., Guo, W., Missimer, T.M., 2006. Aquifer storage and recovery: recent hydrogeological advances and system performance. *Water Environ. Res.* 78 (13), 2428–2435. <https://doi.org/10.2175/106143006x123102>.
- Mumba, M., Thompson, J.R., 2005. Hydrological and ecological impacts of dams on the Kafue Flats floodplain system, southern Zambia. *Phys. Chem. Earth, Parts A/B/C.* 30 (6–7), 442–447. <https://doi.org/10.1016/j.pce.2005.06.009>.
- Neuman, S.P., 1982. Statistical characterization of aquifer heterogeneities: An overview. In: Narasimhan, T.N. (Ed.), *Recent trends in hydrology: Geological Society of America Special Paper*. The Geological Society of America, California, pp. 81–102.
- Neumann, P.E., 2012. Shallow aquifer storage and recovery (SASR): Regional management of underground water storage in hydraulically connected aquifer-stream systems. Master Thesis, Oregon State University, USA.
- Onderka, M., Pecho, J., Nejedlik, P., 2020. On how rainfall characteristics affect the sizing of rain barrels in Slovakia. *J. Hydrol.: Reg. Stud.* 32, 100747 <https://doi.org/10.1016/j.ejrh.2020.100747>.
- Papadopoulos, I.S., Cooper, H.H., 1967. Drawdown in a well of large diameter. *Water Resour. Res.* 3 (1), 241–244. <https://doi.org/10.1029/WR003i001p00241>.
- Pyne, R.D.G., 2005. *Aquifer storage recovery: a guide to groundwater recharge through wells. ASR systems, Florida*, p. 608.
- Richard, S.K., Chesnaux, R., Rouleau, A., Coupe, R.H., 2016. Estimating the reliability of aquifer transmissivity values obtained from specific capacity tests: examples from the Saguenay-Lac-Saint-Jean aquifers, Canada. *Hydrol. Sci. J.* 61 (1), 173–185. <https://doi.org/10.1080/02626667.2014.966720>.
- Rockström, J., Falkenmark, M., 2015. Agriculture: increase water harvesting in Africa. *Nat. N.* 519 (7543), 283. <https://doi.org/10.1038/519283a>.
- Rodell, M., Velicogna, I., Famiglietti, J.S., 2009. Satellite-based estimates of groundwater depletion in India. *Nature* 460 (7258), 999. <https://doi.org/10.1038/nature08238>.
- Roy, A.D., Shah, T., 2002. Socio-ecology of groundwater irrigation in India. In: Llamas, R., Custodio, E. (Eds.), *Intensive use of groundwater challenges and opportunities*. A. A. Balkema publishers, pp. 307–335.
- Runkel, A.C., 1996. Geological investigations applicable to groundwater management, Rochester metropolitan area, Minnesota. Minnesota Geological Survey, St. Paul, Minnesota. Retrieved from the University of Minnesota Digital Conservancy, (<https://hdl.handle.net/11299/122068>).
- Runkel, A.C., Tipping, R.G., Green, J.A., Mossler, J.H., Alexander, S.C., Alexander, E.C., 2003. Hydrogeology of the paleozoic bedrock in southeastern minnesota: minnesota geological survey report of investigations 61. St. Paul, Minn. Retrieved Univ. Minn. Digit. Conserv. (<https://hdl.handle.net/11299/58813>).
- Russo, T.A., Fisher, A.T., Lockwood, B.S., 2015. Assessment of managed aquifer recharge site suitability using a GIS and modeling. *Groundwater* 53 (3), 389–400. <https://doi.org/10.1111/gwat.12213>.
- Sallwey, J., Bonilla Valverde, J.P., Vásquez López, F., Junghanns, R., Stefan, C., 2019. Suitability maps for managed aquifer recharge: a review of multi-criteria decision analysis studies. *Environ. Rev.* 27 (2) <https://doi.org/10.1139/er-2018-0069>.
- Schenk, H.J., Jackson, R.B., 2002. Rooting depths, lateral root spreads and below-ground/above-ground allometries of plants in water-limited ecosystems. *J. Ecol.* 90 (3), 480–494. <https://doi.org/10.1046/j.1365-2745.2002.00682.x>.
- Schoenberg, M.E., 1998. Hydrogeology and sources of recharge to the Buffalo and Wahpeton aquifers in the southern part of the Red River of the North drainage basin, west-central Minnesota and southeastern North Dakota. U. S. Geol. Surv., Minn. <https://doi.org/10.3133/wri974084>.
- Shandilya, R.N., Bresciani, E., Kang, P.K., Lee, S., 2022. Influence of hydrogeological and operational parameters on well pumping capacity. *Journal of Hydrology* 608, 127643. <https://doi.org/10.1016/j.jhydrol.2022.127643>.
- Shiklomanov, I.A., Rodda, J.C., 2003. *World water resources at the beginning of the 21st century. International hydrology series*. Cambridge University Press,, Cambridge.
- Siebert, S., Burke, J., Faures, J.-M., Frenken, K., Hoogeveen, J., Döll, P., Portmann, F.T., 2010. Groundwater use for irrigation—a global inventory. *Hydrol. earth Syst. Sci.* 14 (10), 1863–1880. <https://doi.org/10.5194/hess-14-1863-2010>.
- Smith, W.B., Miller, G.R., Sheng, Z., 2017. Assessing aquifer storage and recovery feasibility in the Gulf Coastal Plains of Texas. *J. Hydrol.: Reg. Stud.* 14, 92–108. <https://doi.org/10.1016/j.ejrh.2017.10.007>.
- Steenberg, J.R., Pettus, M.C., Marshall, K.J., McDonald, J.M., Hamilton, J.D., Chandler, V., 2020. C-49, Geologic atlas of Olmsted County, Minnesota. Minnesota Geological Survey. Retrieved Univ. Minn. Digit. Conserv. (<https://hdl.handle.net/11299/212007>).
- Stefan, C., Ansems, N., 2018. Web-based global inventory of managed aquifer recharge applications. *Sustain. Water Resour. Manag.* 4 (2), 153–162. <https://doi.org/10.1007/s40899-017-0212-6>.
- Szulczewski, M.L., MacMinn, C.W., Herzog, H.J., Juanes, R., 2012. Lifetime of carbon capture and storage as a climate-change mitigation technology. *Proc. Natl. Acad. Sci.* 109 (14), 5185–5189. <https://doi.org/10.1073/pnas.1115347109>.
- Theis, C.V., 1935. The relation between the lowering of the Piezometric surface and the rate and duration of discharge of a well using ground-water storage. *Eos, Trans. Am. Geophys. Union* 16 (2), 519–524. <https://doi.org/10.1029/TR016i002p00519>.
- U. S. Census Bureau, 2019b. Quick Facts Rochester city, Minnesota. [WWW Document]. Accessed on May 20, 2021. URL <https://www.census.gov/quickfacts/table/rochestercityminnesota/PST045219>.
- U. S. Census Bureau, 2019a. Quick Facts Moorhead city, Minnesota. [WWW Document]. Accessed on May 20, 2021. URL <https://www.census.gov/quickfacts/moorheadcityminnesota>.
- Wolf, R.J., 1981. Hydrogeology of the buffalo aquifer, clay and wilkin counties, west-central minnesota. U. S. Geol. Surv., Water Resour. Div. <https://doi.org/10.3133/wri814>.
- Wu, W.-Y., Lo, M.-H., Wada, Y., Famiglietti, J.S., Reager, J.T., Yeh, P.J.F., Ducharne, A., Yang, Z.-L., 2020. Divergent effects of climate change on future groundwater availability in key mid-latitude aquifers. *Nat. Commun.* 11 (1), 1–9. <https://doi.org/10.1038/s41467-020-17581-y>.
- Zoback, M.D., 2007. *Reservoir geomechanics*. Cambridge University Press, New York, p. 490.
- Zuurbier, K.G., Zaadnoordijk, W.J., Stuyfzand, P.J., 2014. How multiple partially penetrating wells improve the freshwater recovery of coastal aquifer storage and recovery (ASR) systems: a field and modeling study. *J. Hydrol.* 509, 430–441. <https://doi.org/10.1016/j.jhydrol.2013.11.057>.